Chalcogenide Letters Vol. 18, No.12, December 2021, p. 797 - 810

Modulating the optoelectronic and thermoelectric properties of chalcopyrite $AgXTe_2$ (X: Ga, In) via in-plane biaxial strain

A. Shahzad[a], M. Kashif[a,*], Ateeq-ur-Rehman[b], K. Kamran[b] S. Ghani[c], M. S. Shifa[d] M. Yaseen[b]

[a]*Physics Department, Govt College University Faisalabad (GCUF),Allama Iqbal Road, Faisalabad 38000, Pakistan*

[b]*Department of Physics, University of Agriculture, Faisalabad, Pakistan*

[c]*Department of Physics, University of Engineering and Technology (UET) Lahore, Pakistan*

[d]*Institute of Physics, The Islamia University of Bahawalpur, Bahawalpur, Pakistan*

The influence of biaxial-in-plan strain on optoelectronic and thermoelectric characteristics of $AgXTe_2$ (X: Ga, In) chalcopyrite type compound has been investigated using density function theory base on full potential linear augmented plane wave technique. The generalized Perdew-Burke-Ernzerhof gradient approximation (PBEsol GGA) is used to optimize unit cell and the Tran-Blaha modified Becke-Johnson (TB-mBJ) approach is employed to improve the electronic, optical and thermoelectric properties. The effects of biaxial strains of the tensile (1%, 2%, 3%) and compression (-1%, -2%, -3%) have been calculated along with contribution of two cations (Ga and In). The calculated band gap of $AgGaTe_2$ and $AgInTe_2$ without strain is 1.17 and 1.13 eV that decreases with applied tensile strain and increases with compressive strain. Without strain maximum absorption is obtained at 1.3 eV and 1.1 eV $AgGaTe_2$ and $AgInTe_2$ respectively, however, tensile and compressive strain shows red and blue shift accordingly. The increase in flatness of valance band with compressive strain results in a large Seebeck coefficient due the large hole effective mass. This identifies $AgGaTe_2$ as a possible efficient thermoelectric material. Consequently, the present study is very useful for developments of desired characteristics by applying strain for optoelectronic and thermoelectric devices.

(Received September 21, 2021; Accepted December 14, 2021)

Keywords: First principles calculation, biaxial-in-plan strain, electronic properties, optical properties, thermoelectric properties

1. Introduction

Renewable and efficient energy source is one of the biggest challenges for human and global environment. The solar energy conversion technologies are entering into a new regime with inception of novel device architectures, nanotechnologies and new materials for the device. The solar energy is best alternative source of sustainable energy supply than fossil energy because it is

[*] Corresponding author: mkashif@gcuf.edu.pk

https://doi.org/10.15251/CL.2021.1812.797

considered to be everlasting on human time scale and does not affect the environment in any way. Compared to their binary analogues, the ternary chalcopyrite compounds of I-III-VI2 and II-VI-V2 families are considered to be promising compounds for investigation of optoelectronics, non-linear optical devices, solar cells, light emitting diodes and solid-state laser systems because of high absorption rate in visible region, wider band gap and small melting points. From family of I-III-VI2, the Ag-based ternary chalcopyrite compound is a potential candidate for many optoelectronic devices [1-6].

Hahn et al [7] is the first one who discovered and reported the properties of I-III-VI2 compounds. The semiconductor nature of ternary chalcopyrite compounds was described by Goodman et al. [8]. Photoelectric conversion using these compounds was done by Tuttle et al [9]. Lazewski et al [10] and Alonso et al [11] calculated the electronic, elastic and complex dielectric properties of these compounds respectively.

The I-III-VI2 chalcopyrite compounds are also good thermoelectric materials. However, their usage as thermoelectric device is limited due to low efficiency [12]. Thermoelectric materials are a green energy or renewable energy source which converts the wasted heat from the environment into useful electrical energy without polluting the environment. They have potential applications in waste-heat recovery, air conditioning and refrigerators. Therefore, now a days many researchers all over the world are engaging in this effort to explore new efficient thermoelectric materials and enhancing the efficiency of existing thermoelectric materials [13-18]. Noticing them, the $AgXTe_2$(X=Ga, In) chalcopyrite has paying much attention due to its fascinating properties of structural, electronic, optical and thermoelectric properties of this compound has been extensively study both theoretically as well as experimentally [19-22].

Estimating the features and qualities of new compounds earlier than fabrication is one of the greatest achievements of modern computational and theoretical method. This helps in saving very expensive and rare materials, energy, time, money and most important shields the atmosphere from polluting.

Utilizing strain is a practical strategy to tune and control the physical and chemical properties of nanomaterials by changing structural parameters. Recent studies on low dimensional materials shows that electronic, optical, magnetic, mechanical, and thermal characteristics of nanomaterials can all be improved due to exclusive layered structures and bond symmetry by strain causing methods [23-25]. These strain-induced processes and their utilization put emphasis on strain engineering.

In this article we have been investigated the effect of biaxial in plane strain on structural, electronic, optical and thermoelectric properties on ternary chalcopyrite $AgXTe_2$(X=Ga, In) compounds based on many electrons system. Tensile as well as compressive strain study have been applied to find the effect on band structures, absorption coefficient and figure of merit. Furthermore, to my best knowledge and to the reported experimental and theoretical survey, there is no studies on biaxial in-plane strain induced variations on ternary chalcopyrite $AgXTe_2$ (X=Ga, In) compounds.

2. Computational Methodology

First principle calculation to study the electronic, optical and thermoelectric properties of $AgXTe_2$(X=Ga, In) compounds under strain were performed by using full potential linearized

augmented plane wave (FP-LAPW) method implemented in the WIEN2K code. The generalized gradient approximation (GGA) within Perdew-Burk-Ezrenhop (PBE) method are used for the exchange correlation potential to study the structural and electronic properties. These GGA based calculation gives the underestimation of band gap therefore modified Trans Blah – Becke Johnson (Tb-mbj) potential was use to obtained the accurate band gap. Cutoff energy to separate the core and valance states are set to be -6.5Ry. Muffin tin radius are taken for Ag = 2.5a.u , Ga = 2.5a.u , In = 2.5a.u and for Te= 2.06a.u. The plane wave cutoff was defined as $R_{mt} \times K_{max} = 7$. Self consistency was achieved by using 1000 k-points in irreducible Brillion zone and total energy is converged to within 10^{-4}Ry. The in-plane biaxial strain is defined by

$$\varepsilon_a = \frac{a - a_0}{a_0} \tag{1}$$

where a_0 is optimized in-plane lattice constant for the unstrained case and a is the in-plane lattice constant for the strained case. The thermoelectric properties of $AgXTe_2$(X=Ga, In) compounds under strain were calculated on the basis of semiclassical Boltzman Transport theory within the constant scattering time approximation (CSTA) by using BoltzTrap Code. For thermoelectric properties measurement a dense mesh of 30,000 k points is used.

3. Results and Discussion

In this research work, we report the effect of biaxial in-plane strain on the properties of ternary chalcopyrite $AgXTe_2$(X=Ga, In) compounds. For this purpose, we evaluated the effect of strain on equilibrium lattice constant, band gap value, absorption coefficient and thermoelectric properties.

3.1. Structural Properties

At ambient temperature and pressure, the ternary chalcopyrite $AgXTe_2$(X=Ga, In) has rutile tetragonal phase with space group $I-\overline{4}2d(No.1\,22)$. The primitive unit cell of $AgXTe_2$(X=Ga, In), contain four formula unit atoms, Ag, (X=Ga, In) and two Te atoms at positions (0,0,0), (0, 0, 1/2), (0.26, 1/4, 1/8), respectively [27-29]. The crystal structure of $AgXTe_2$(X=Ga, In), is shown in Fig.1.

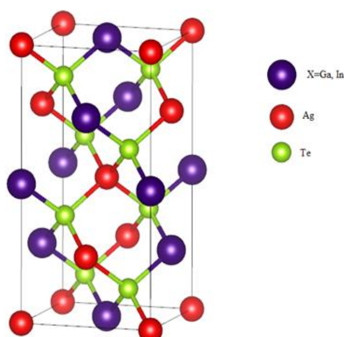

Fig. 1. Rutile tetragonal structure of $AgXTe_2$(X=Ga, In).

The ternary chalcopyrite $AgXTe_2$(X=Ga, In) is not perfect tetrahedral crystal structure due to the tetragonal distortion parameter $\eta = c/2a \neq 1$ and the anion displacement parameter $u \neq ¼$. By interaction of neighboring atoms in crystal, the distortion in structure is produced due to shifting of anions from their ideal positions with an amount of anion displacement (u) and it can be calculated with this equation.

$$u = \frac{1}{2} - \left[\frac{c^2}{32a^2} - \frac{1}{16} \right]^{\frac{1}{2}} \tag{2}$$

These structural distortion are negligible but have significant importance in describing the electronic properties of ternary chalcopyrite.

The optimized lattice constant of $AgInTe_2$ and $AgGaTe_2$ under unstrained case are a = 6.431Å, c = 12.770Å, and a = 6.415Å, c = 12.323 Å, respectively which are very close to the experimental values indicating our optimized results are reliable. The optimized lattice parameters of $AgXTe_2$(X=Ga, In) under various strains are listed in Table 1.

Table 1. Structural properties of $AgGaTe_2$ and $AgInTe_2$ with tensile and compressive strain.

strain	Lattice parameters (Å)	Calculated Parameters This work		Previous Theoretical work [30]		Experimental Parameters [30]	
		$AgGaTe_2$	$AgInTe_2$	$AgGaTe_2$	$AgInTe_2$	$AgGaTe_2$	$AgInTe_2$
0%	a c c/a	6.414 12.322 1.921	6.431 12.77 1.985	6.469 12.284 1.8989	6.623 12.988 1.961	6.288 11.940 1.898	6.467 12.633 1.953
Tensile Strained applied							
1%	a c c/a	6.478 12.322 1.902	6.494 12.770 1.966				
2%	a c c/a	6.542 12.322 1.883	6.559 12.770 1.946				
3%	a c c/a	6.606 12.322 1.865	6.623 12.770 1.928				
Compressive strained applied							
-1%	a c c/a	6.3504 12.322 1.940	6.3662 12.77 2.00				
-2%	a c c/a	6.286 12.322 1.960	6.302 12.770 2.020				

-3%	a	6.222	6.237		
	c	12.322	12.770		
	c/a	1.980	2.040		

2.2. Electronic Properties

Fig.2 (a) and (b) shows the electronic band structures obtained from our Tb-MBj simulations for the unstrain $AgGaTe_2$ and $AgInTe_2$ respectively. As shown in Fig.2 (a) and (b) without strain $AgGaTe_2$ and $AgInTe_2$ are direct band-gap semiconductor with a band gap of 1.173 eV and 1.13 eV using Tb-mbj functional which is in a good agreement with previous works. From the band structure graphs it can be seen that the valance band maximum (VBM) and conduction band minimum (CBM) is located on the Γ point. Band structure plots under different biaxial compressive and tensile strain conditions are shown in Fig.2 (c) and (d) It can be seen that tensile and compressive strains does not change the nature of direct semiconducting band gap.

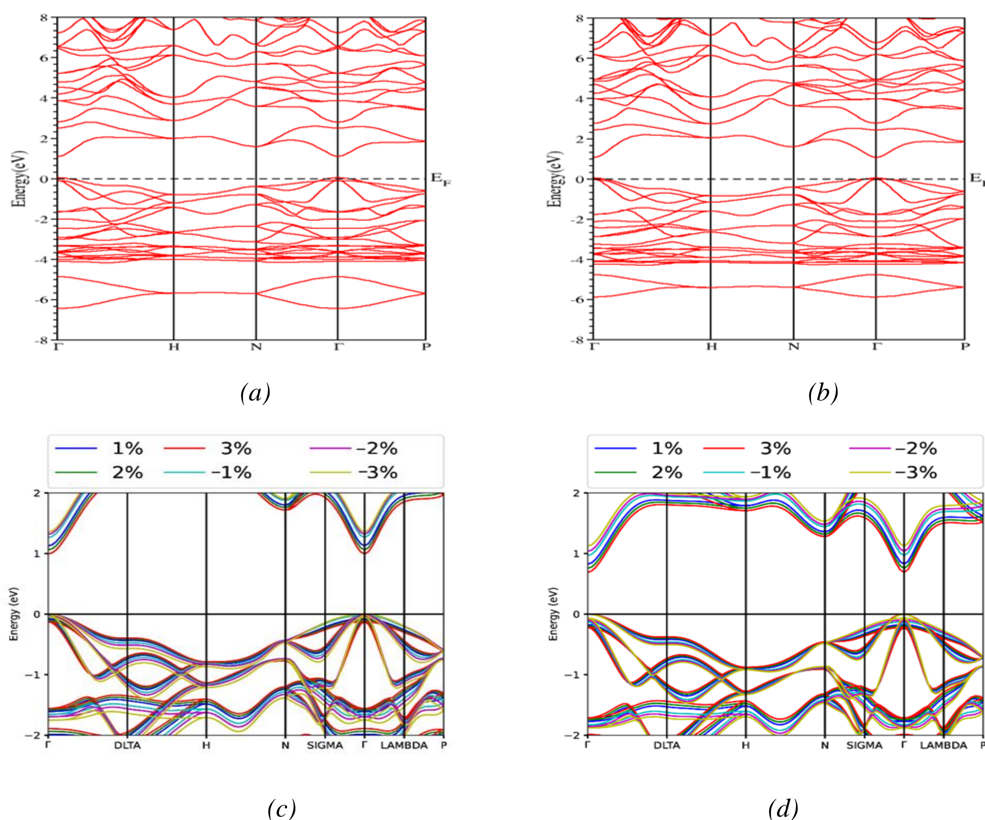

Fig.2. Band structures of $AgGaTe_2$ and $AgInTe_2$ (a) and (b) unstrained and (c) and (d) for different compressive and tensile strained, respectively.

It is observed that band gap increases for the compressive strain cases, while it decreases in the case of the tensile stress. Fig.3 represent the variation of band gap under different biaxial compressive and tensile strain conditions. Band structures plots shows that under tensile strain CBM move downward while for compressive strain move upward with respect to fermi level therefore reduction in band gap for tensile strain cases and vice versa for compressive strain cases.

Our results show that through applying biaxial compressive and tensile strains on $AgGaTe_2$ and $AgInTe_2$, the band gap of $AgGaTe_2$ and $AgInTe_2$ can be continuously modulate with different magnitude of strains.

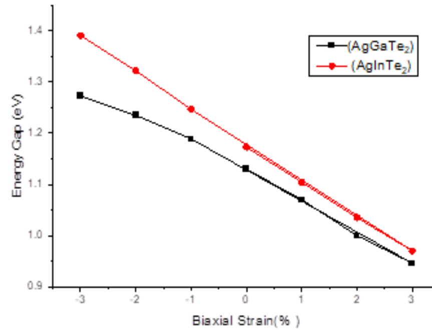

Fig. 3. The variation of energy band gap with strain.

To get further insight for the understanding of strain on the electronic structure total (TDOS) and partial density of states (PDOS) are calculated and Dos plots of $AgGaTe_2$ and $AglnTe_2$ without strain are shown in Fig.4. From the PDOS plots it is observed that VBM is mainly composed of Te-p and Ga-p states in case of $AgGaTe_2$ similarly for $AgInTe_2$ VBM is mainly composed of Te-p and In-p states. Above Fermi energy, in conduction band minima (CBM) the maximum contribution comes from Ga-s, In-s and Te-p states. Overall, the trend of DOS of $AgGaTe_2$ and $AgInTe_2$ compounds considered to be similar.

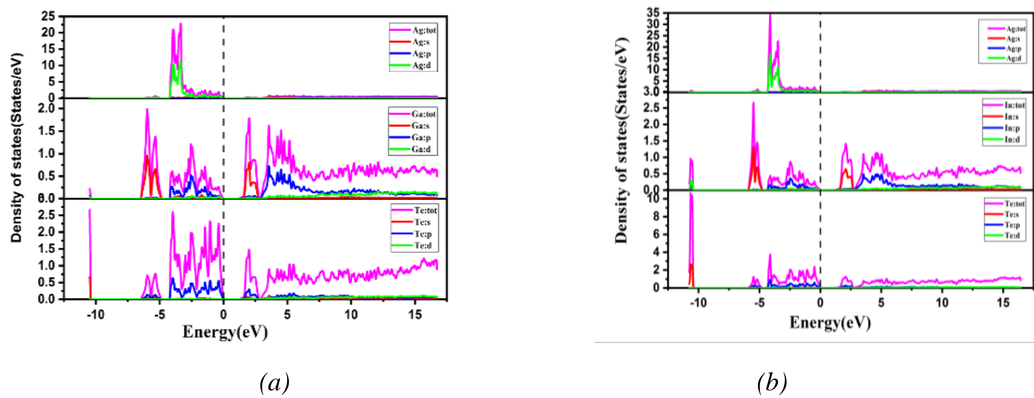

(a) *(b)*

Fig. 4. Partial density of states of (a) $AgGaTe_2$ (b) $AglnTe_2$.

To explore the influence of compressive as well as tensile strain on total density of states it is observed that for the tensile strain case the VBM is going toward lower energy states and CBM is shifting toward fermi level. In case of compressive strain, VBM is shifting toward Fermi level and CBM moves toward higher energy states. From total DOS as shown in Fig.5 (a-d), we also noted that, in tensile strain the gap between VBM to CBM is reducing but in compressive strain its value is increasing respectively.

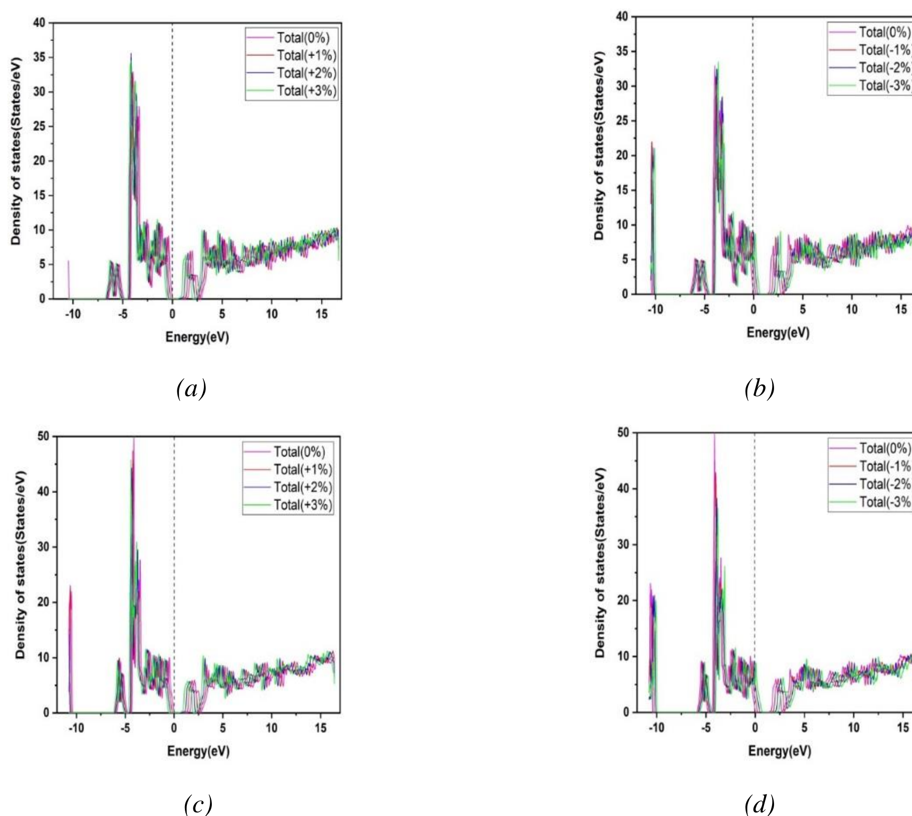

(a) (b)

(c) (d)

Fig. 5. Partial density of states of (a) $AgInTe_2$,(0%), (b) $AgInTe_2$ (1 ,-1)%, (c) $AgInTe_2$ (2 ,-2)% and (d) $AgInTe_2$ (3 ,-3)% for Tensile and Compressive Strained, respectively.

3.3. Optical Properties

The study of optical spectra is very important from practical point of view of optical properties in different devices such as solar cell, LEDs, modulators and nonlinear optics. The optical property of material is denoted by complex dielectric function ε (ω)

$$\varepsilon(\omega) = \varepsilon_1(\omega) + i\varepsilon_2(\omega) \quad (3)$$

which represents electron and photon interaction. $\varepsilon_1(\omega)$ and $\varepsilon_2(\omega)$ denotes its real and imaginary parts. Other optical parameters like refractive index n(ω), absorption coefficient α(ω) and optical conductivity σ (ω) can also be measured with the help of dielectric function.

Fig.6 (a-d) represents the real and imaginary parts of dielectric functions for $AgGaTe_2$ and $AgInTe_2$ with and without strain. From real part of dielectric function in Fig.6 (a) and (b) it is observed that transition of electron from valence to conduction band occurs at 2.1 eV and 2.23eV for $AgGaTe_2$ and $AgInTe_2$ respectively, and $\varepsilon_1(\omega)$ further decreases up to 5.2 eV and 6.7 eV for $AgGaTe_2$ and $AgInTe_2$ respectively for unstrained materials. By applying the tensile strain, value of the real part of dielectric function reduces while for compressive strain its value increases. This behavior is mainly due to the fact that compressive strain increases the electric polarization while the tensile strain decreases the electric polarization. Fig.6 (a) and (b) also indicate that for each compound the value of ε1 is negative for higher values of energy which indicate the metallic reflectivity of $AgXTe_2$ (X= Ga, In) in this region.

Fig.6 (c) represents the imaginary part of the dielectric function of $AgInTe_2$ while the Fig.6 (d) represents the imaginary part of the dielectric function of $AgGaTe_2$. From these figures it can be observed that as the tensile strain increases, the imaginary part of the dielectric function slightly move towards the red end of the spectrum because the direct band gap of $AgXTe_2$ (X= Ga, In) is decreasing under tensile strain, while as the compressive strain increases it showed the blue shift because of its direct band gap is increasing under compressive strain. Moreover, it is observed from Fig.6 (c) and (d) both the compounds have maximum absorption takes place in the UV region however a remarkable absorption also takes place in the visible region. In the visible region (1.65-3.1eV), as we increase the value of tensile strain, the peak value of ε_2 of $AgXTe_2$ (X= Ga, In) enhances, which indicates that by applying the tensile strain the transition probability of electrons can increases while the compressive strain has the reciprocal effect on the transition probability in this region. In UV region (3.2 to 30 eV), the increase in compressive strain increases the transition probability while the tensile strain reduces the transition probability.

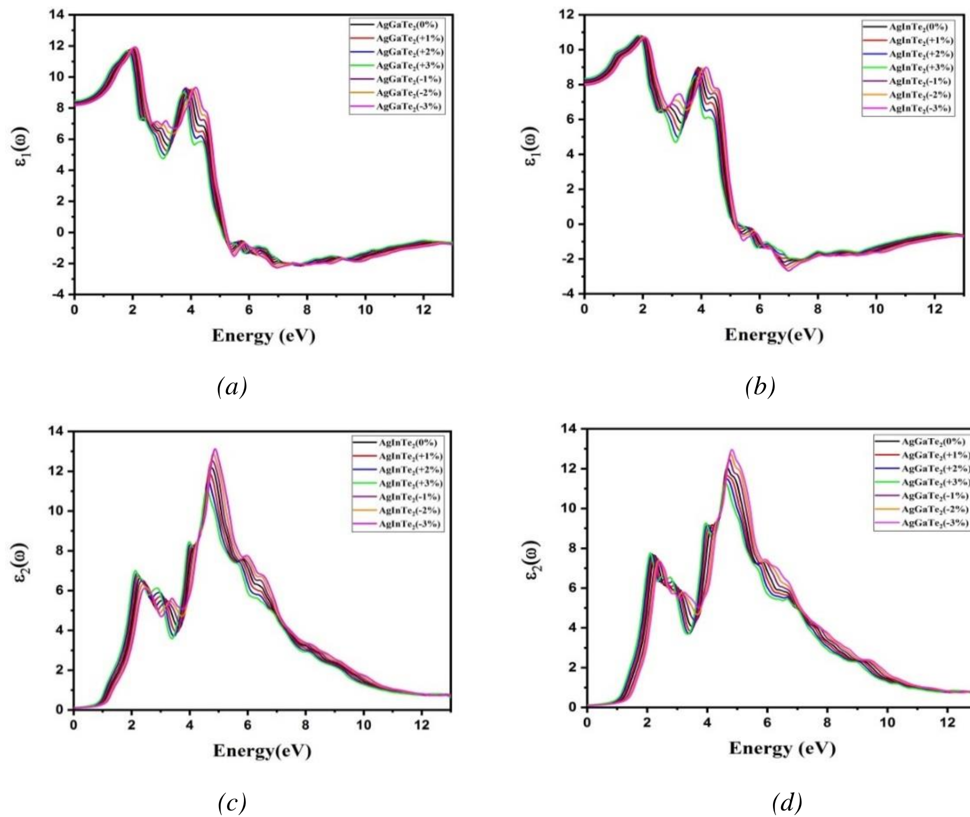

Fig. 6. (a-b) Real and (c-d) Imaginary Parts of $AgGaTe_2$ and $AgInTe_2$ with and without strain, respectively.

Measurement of the attenuation in the amount of light intensity per unit of length is known as absorption coefficient. The behavior of absorption coefficients of $AgXTe_2$ (X=Ga, In) with and without different strains is shown in Fig.7 (a-d) The results obtained by the plot of absorption coefficient of both the compounds are consistent with the results obtained by the plots of imaginary part of the dielectric function. From Fig.7 (b & d), it is noted that when increases the tensile as well as compressive strain the absorption coefficient has at zero level in the energy range 0.0 to 1.0 eV. From absorption spectra, we noted that the absorption edges are positioned at 1.3 eV and 1.1 eV for

$AgGaTe_2$ and $AgInTe_2$ respectively. This shows that $AgXTe_2$ (X=Ga, In) are brilliant mid-IR transparent compounds for small energy photons and displays zero absorption coefficient in that region. When energy increases more than absorption edge value, the absorption increases. The absorption coefficient again decreases in high energy region, and this is the distinctive nature of semiconductor. Even if the beginning of absorption is the visible region, however maximum absoption takes place in UV region. Moreover, in visible region using tensile and compressive strains for $AgXTe_2$ (X=Ga, In), the absorption peaks show red and blue shift respectively. Apart from this, strains also change the peak intensity slightly, the peak maxima of absorption coefficient of $AgXTe_2$ (X=Ga, In) is observed under tensile strain of +3% and peak minima is observed at -3 % magnitude of compressive strain, which shows the tranparency of these materials is more for compressive strain as compare to tensile strain but in UV region, compressive strain have maximum absorption coefficient and tensile strains have less absorption rate.

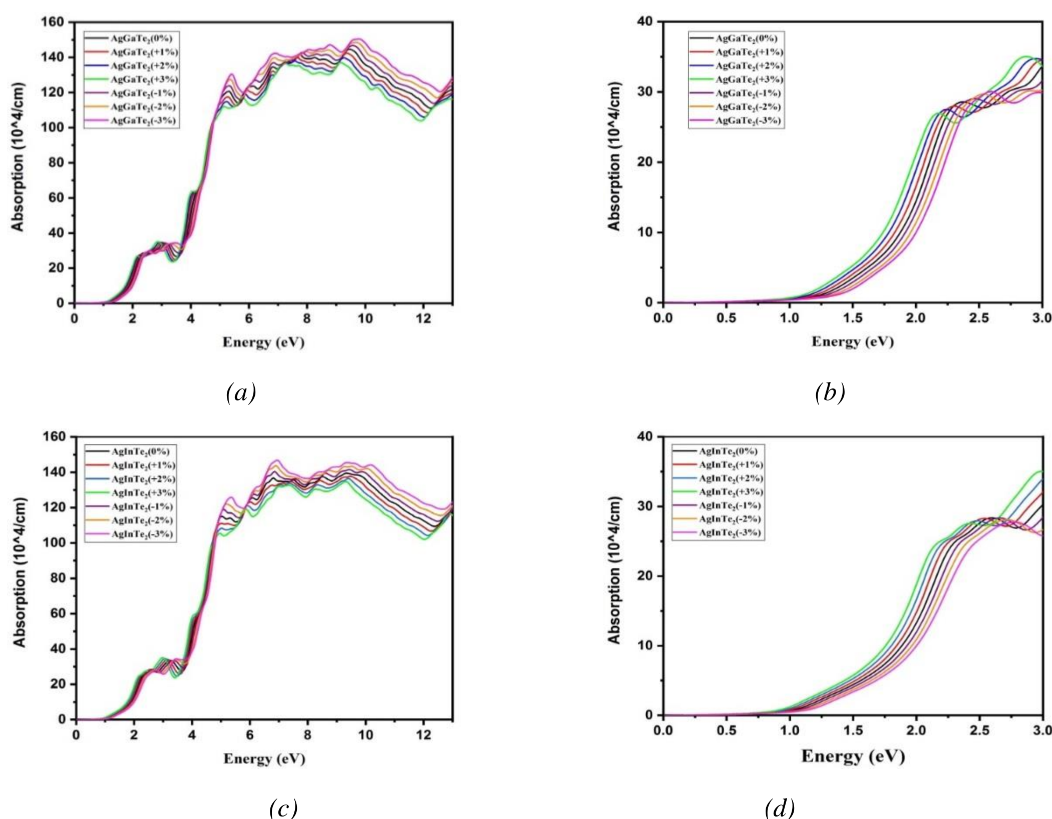

Fig. 7. Absorption Coefficient of $AgGaTe_2$ (a,b) and $AgInTe_2$ (c,d) with and without strain respectively.

The study of optical conductivity parameter is important because this phenomenon is associated with photo-electric conversion ability and essentially used to find the variation produced by light. Fig. 8(a & b) represent the optical conductivity of $AgXTe_2$ (X=Ga, In) for different values of strain. Fig. 8(a & b) indicate that for low energy values the effect of strain on optical conductivity of each compound is negligible. However, these compounds have non-zero values in visible region (1.65- 3.1 eV), therefore can be used in optoelectronic devices. It is noted from figures that tensile and compressive strains do not have any major influence on the optical spectra of the compounds. The applied strains just change the intensity of the peaks slightly. Consequently, applying

compressive strain give rise to intensity of peaks and hence conductivity increases for both visible and UV region. However, the peak intensity as well as conductivity decrease by applying tensile strain. This is because by the application of tensile strain the inter atomic distance as well as the bond length increases but the charge density reduces which in turn result in the reduction of the transition probability between valance and conduction band electrons.

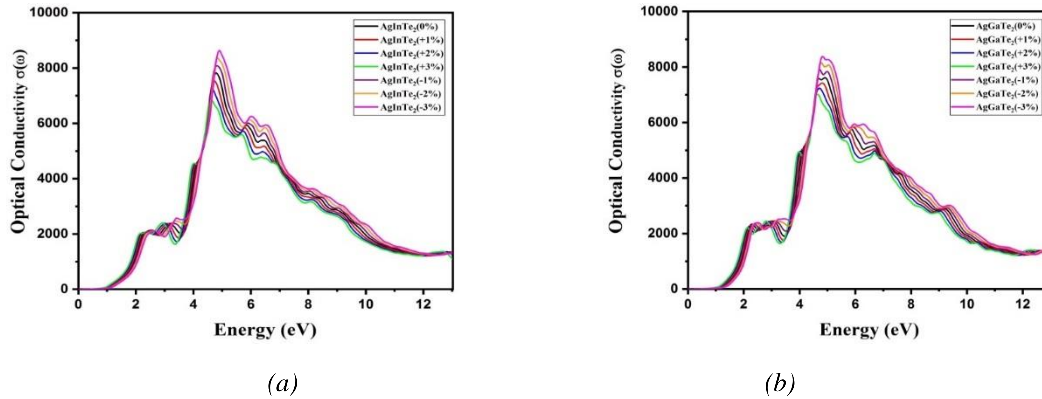

(a) *(b)*

Fig. 8. Optical Conductivity of (a)$AgInTe_2$ and (b)$AgGaTe_2$ with and without strain respectively.

3.4. Thermoelectric Properties

Thermoelectric materials are the best choice to convert heat into electrical energy. The thermoelectric power generation between heat and electricity is measured by the dimensionless Figure of merit (ZT). The ZT value is defined as: $ZT = S^2\sigma T/\kappa$. Here, S is Seebeck coefficient, $PF = S^2\sigma$, is power factor,σ is electrical conductivity and κ is thermal conductivity. The improvement in ZT value can be done by increasing power factor or decreasing thermal conductivity. Figure of merit must be fulfill that condition ($ZT \geq 1$). A large value of PF suggests that electrons are efficient to convert heat into electricity, whereas we need a very low value of thermal conductivity to tolerate temperature gradient. To achieve a high value of ZT requires simultaneously high Seebeck coefficient, high electrical conductivity but sustain very low thermal conductivity, which is very challenging because these demands are often contrasting to each other in conventional materials as, the Seebeck coefficient decreases and electrical conductivity improves with carrier concentration but corresponding thermal conductivity also rises with carrier concentration. Presence of nearly flat bands around the Fermi level for all the values of applied strain indicate that $AgXTe_2$ (X=Ga, In) can be favorable contenders for TE applications.

Fig.9 (a) and (b) shows the temperature dependent Seebeck coefficient of $AgGaTe_2$ and $AgInTe_2$ under different strains. The calculated Seebeck coefficient of unstrained for $AgGaTe_2$ and $AgInTe_2$ at 200K is 1400 μV/K and 1600 μV/K respectively. It is observed that both the compounds have positive Seebeck coefficient, positive value of Seebeck coefficient referred that the charge carrier are holes so both the compounds are of p type, which expected that $AgXTe_2$ (X=Ga, In) compounds stand good for thermoelectric materials at higher temperature.

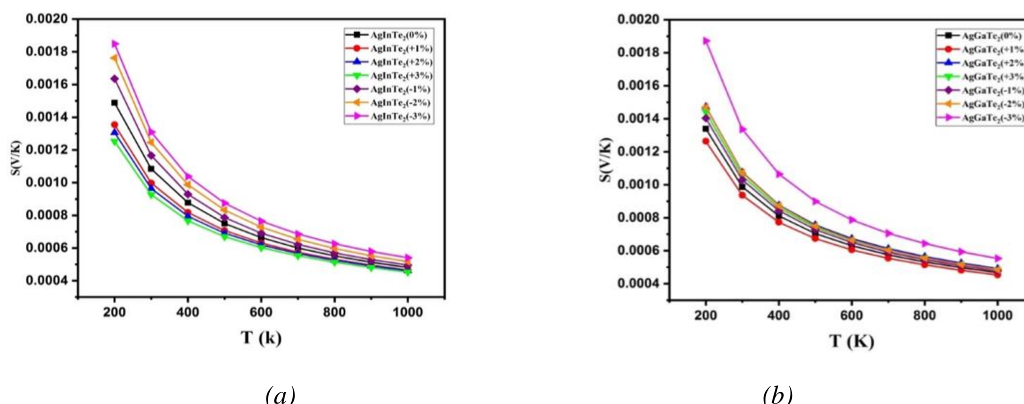

(a) *(b)*

Fig. 9. Variation of Seebeck Coefficient with temperature of (a)$AgInTe_2$ and (b)$AgGaTe_2$.

It can be seen that the increase in temperature leads to decrease the Seebeck coefficient, meanwhile the Seebeck coefficient enhances with increase in strain both compressive and tensile. The variation of strain dependent Seebeck coefficient is consistent with prediction from the analysis of results of band structure and DOS under strain. This increase in the Seebeck coefficient is attributed to similarity of their band dispersions around the fermi level. The flatness of the upper valence bands at the gamma point gives large hole effective mass. This large hole effective mass is significant for the thermoelectric performance of materials such small hole effective mass gives good electrical conductivity and large effective mass give large Seebeck coefficient for the p-type compounds.

From the Fig .9 it can be observed for the same temperature the Seebeck coefficient increases as with the increase in compressive strain because as from the band structure graphs it can be seen that the top of valence bands at the gamma point are flat and this flatness increases with increasing the compressive strain. For $AgGaTe_2$ and $AgInTe_2$, the value of Seebeck coefficient for -3% compressive strain is 1900 μV/K and 1850 μV/K respectively.

The variation of electrical conductivity (σ/τ) Vs T is shown in Fig. 10 (a) and (b) for $AgGaTe_2$ and $AgInTe_2$ respectively. The electrical conductivities of $AgXTe_2$ (X=Ga, In) increases with increasing the temperature showing the semiconductor like temperature dependance. For each given temperature the electrical conductivity decreases with strain changes from tensile to compressive for both $AgGaTe_2$ and $AgInTe_2$. The unstrained compounds of $AgGaTe_2$ and $AgInTe_2$ have electrical conductivity of 6.3×10^{17} 1/ Ωm.s and 6.4×10^{17} 1/ Ωm.s respectively at 1000 K.

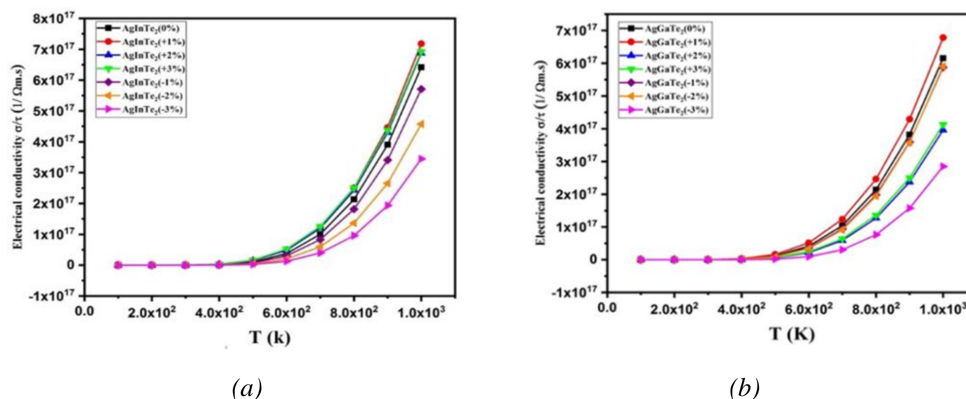

(a) *(b)*

Fig. 10. Variation of Electronic Conductivity with temperature of (a)$AgInTe_2$ and (b)$AgGaTe_2$.

The PF can be calculated by Seebeck coefficient and electrical conductivity. The variation of PF with temperature along the strain is shown in Fig. 11(a) and (b) it is observed from graphs that Power factor improves by increasing temperature. It can be seen the PF of both the compounds remain unchanged by applying strain up to 300K. Above 400K there is an exponential rise in the value of PF for each value of applied strain. However, for the rise of +1% strain both the compounds attain the highest value of PF. For $AgInTe_2$, the unstrained value of PF is 1.5×10^{11} W/mk^2s and the highest value is 1.6×10^{11} W/mk^2s at +1% tensile strain. By applying compressive strain, PF decreases.

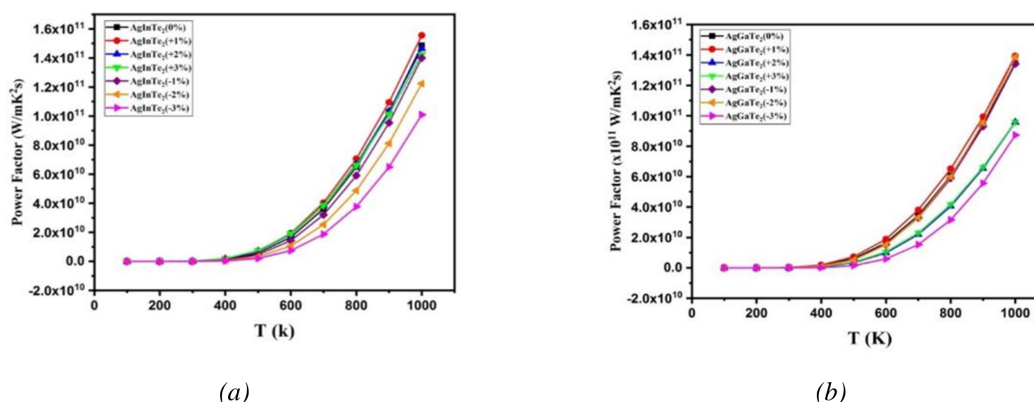

(a) *(b)*

Fig. 11. Variation of power factor with temperature of (a)$AgInTe_2$ and (b)$AgGaTe_2$.

4. Conclusion

In summary, we have investigated the effect of biaxial in plane strain on electronic, optical and thermoelectric properties of $AgXTe_2$ (X: Ga, In). Our calculations shows that the strain strongly affects the band gap of $AgXTe_2$ (X: Ga, In) but under all strain values shows the direct band gap semiconducting nature. The absorption spectra show red and blue shifting with the tensile and compressive strain. The increase in flatness of valance band with compressive strain results in a large Seebeck coefficient due the large hole effective mass. The effect of strain on the electro-optical and transport properties of $AgXTe_2$ (X: Ga, In) can offer useful guidelines to design thermoelectric and photovoltaic materials.

Acknowledgments

The computational facilities for this work were provided by Department of Physics, Govt College University Faisalabad and Department of Physics, University OF Agriculture Faisalabad.

References

[1] X. Z. Zhang, K. S. Shen, Z. Y. Jiao, X. F. Huang, Computational and Theoretical Chemistry **1010**, 67 (2013).

[2] G. Morell, R. S. Katiyar, S. Z. Weisz, T. Walter, H. W. Schock, I. Balberg, Applied physics letters **697**, 987 (1996).
[3] T. Raadik, J. Krustok, M. V. Yakushev Phys. B Condens. Matter **406**, 418 (2011).
[4] A. Jagomägi, J. Krustok, J. Raudoja, M. Grossberg, OjaI, M. Krunks and M. Danilson, Thin Solid Films **480**, 246 (2005).
[5] M. Benabdeslem, H. Sehli, S. Rahal, N. Benslim, L. Bechiri, A. Djekoun, T .Touam, Boujnah M. El, A. Kenz, A. Benyoussef, X. Portier, Journal of Electronic Materials **45**, 1035 (2016).
[6] D. Xue, K. Betzler and H. Hesse, Physical Review B. **62**, 13546 (2000).
[7] H. Hahn, G. Frank, W. Klingler, A. Meyer, G. Stroger, Z. Anorg. Chem. **271**, 153 (1953).
[8] C. H. L. Goodman and R. W. Douglas, Physica **20**, 1107 (1954).
[9] J. R. Tuttle, M. A. Contreras, T. J. Gillespie, K. R. Ramanathan, A. L. Tennant, J. Keane, A. M. Gabor, R. Noufi, Prog. Photovolt. – accelerated communication **3**, 235 (1995).
[10] J. Łażewski, H. Neumann, P. T. Jochym and K. Parlinski, Journal of applied physics **93**, 3789 (2003).
[11] M. I. Alonso, K. Wakita, J .Pascual, M. Garriga, N. Yamamoto, Phys. Rev. B **63**, 075203 (2001).
[12] A. Charoenphakdee, K. Kurosaki, H. Muta, M. Uno, S. Yamanaka, Mater. Trans. **50**, 1603 (2009).
[13] J. P. Heremans, Nature **508**, 7496 (2014).
[14] J. S. Rhyee, K. H. Lee, S. M. Lee, E. Cho, S. I. Kim, E. Lee, Y. S. Kwon, J. H. Shim, G. Kotliar, Nature **459**, 965 (2009).
[15] S. N. H. Eliassen, A. Katre, G. K. H. Madsen, C. Persson, O. M. Løvvik, K. Berland, Phys. Rev. B. **95**, 045202 (2017).
[16] G. D. Mahan, Phys. Rev. B. Condens. Matter Mater. Phys. **87**, 045415 (2013).
[17] D. Kaczorowski, K. Gofryk, Solid State Commun. **138**, 337 (2006).
[18] N. Miao, B. Xu, N. C. Bristowe, D. I. Bilc, M. J. Verstraete, P. Ghosez J. Phys. Chem. C **120**, 9112 (2016).
[19] K. M. Wong, W. K. Chim, J. Q. Huang, L. Zhu, J. Appl. Phys. **103**, 054505 (2008).
[20] S. Ullah, H. U. Din, G. Murtaza, T. Ouahrani, R. Khenata, S. B. Omran, Journal of Alloys and Compounds **617**, 575 (2014).
[21] W. Wu, K. Wu, Z. Ma, R. Sa, Chemical Physics Letters **537**, 62(2012).
[22] S. Arai, S. Ozaki, S. Adachi, Applied optics. **495**, 829 (2010) .
[23] Y. Sun, C. Wang, L. Chu, Y. Wen, Y. Na, M. Nie, X. Chen, Solid State Commun. **152**, 446(2012).
[24] Z. Li, I. A. Kinloch, R. J. Young, K. S. Novoselov, G. Anagnostopoulos, J. Parthenios, C. Galiotis, K. Papagelis, C. Y. Lu, L. Britnell, ACS Nano **9**, 3917 (2015).
[25] J. D. Baran, M. Molinari, N. Kulwongwit, F. Azough, R. Freer, D. Kepaptsoglou, Q. M. Ramasse, S. C. Parker, J. Phys. Chem. C. **119**, 21818 (2015).
[26] S. R. Zhang, L. H. Xie, X. W. Chen, Z. G. Shia, K. H. Song, Chalcogenide Letters **11**(8), 373(2014).
[27] R. Mahdjoubi, Y. Megdoud, L. Tairi, H. Meradji, Z. Chouahda, S. Ghemid, El Haj F. Hassan, International Journal of Modern Physics B **33**, 071950045 (2019).
[28] J. Zhang, Y. C. Zhou, Z. S. Ma, L. Q. Sun, P. Peng, Int J Hydrogen Energy **38**, 3661e9 (2013)

[29] M. Kashif, T. Munir, N. Nasir, M. Sharif, A. Shahzad, T. Ahmad, A. Hussain, M. Noreen, Dig. J. Nanomater. Bios **14**, 137 (2019).
[30] H. Xiao, J. Tahir-Kheli, W. A. Goddard, The Journal of Physical Chemistry Letters **2**, 212 (2011).